2D TIME AVERAGED FLOW MAPPING OF DIE ENTRY IN FLOW OF HIGHLY CONCENTRATED SHEAR-THINNING AND SHEAR-THICKENING SUSPENSIONS

Boris Ouriev (Ur'ev)

Bühler AG, Uzwil, CH-9244, Switzerland, e-mail: boris.ouriev@buhlergroup.com

Keywords: Channel flow; Fluid flow; Two-dimensional flow map; Non-Newtonian fluid; Concentrated suspension; Elongation flow; Die entry; Shear-thickening; Shear-thinning; Ultrasound Doppler

ABSTRACT

In this work a methodology for high-resolution time averaged 2D flow mapping (e.g. Takeda, 1999) of converging flows was explored. Flow of non-transparent, highly concentrated shear-thinning and shear-thickening suspensions was circulating through the entrance flow adapter with the adjustable position of the die entry. The entrance region was scanned with the distance resolution of 2.7 x 1 mm, radial to axial displacement respectively. Time averaged flow map was composed from 1D flow profiles measured along the ultrasonic sensor beam using Ultrasonic Pulsed Echo Doppler technique (UVP product of Met-Flow SA, e.g. Takeda 1986, 1991, 1995). Priory to die entry visualization an investigation of flow properties was performed using a novel in-line non-invasive measuring technique. The method is based on combination of the UVP velocity monitoring and pressure difference (PD) method (e.g. Windhab et. al., 1996 and Ouriev, 2000, Ouriev et. al. 1995, 1998, 1999, 2002). The rheological flow properties were derived from simultaneous recording and on-line analysis of the velocity profiles across the tube channel and related radial shear stress profiles calculated from the pressure loss along the flow channel. Comparison between flow of mentioned above model suspensions was qualitatively analyzed. For the first time the flow divergence of shear-thickening suspension could be visualized. From comparison between entrance flow of viscous shear-thinning and shear-thickening suspensions a strong viscoelastisity of shear-thickening suspensions in elongation flow has been proposed. This method opens an opportunity of precise flow mapping of viscoelastic and viscous, non-transparent and highly concentrated fluids. This is important for industrial type of fluid processing machinery, where characteristics of elongation flow (flow geometry) has global impact on quality of fluid processing.

1. INTRODUCTION

Highly concentrated suspensions play important technological role in various branches of industry as food, chemistry, pharmaceutics, cosmetics, ceramics, paper and etc. Traditionally, knowledge gained in rheological studies using off-line rheometers is transferred to "real" flow situations in different types of flow processes. According to study of Uriev (1980, 1988, 1992) a close relationship between rheology, microstructure and fluid macro properties can be drawn (e.g. Windhab, 1986). In that contact in-line rheological measurement of suspensions flow become one of first priority solutions on the way to improved process control especially if elongation type of flow is concern.

In present work the advantages of relatively small ultrasound and pressure sensor dimensions and the ability of ultrasound to propagate through the solid walls and opaque fluids was used.

A detailed study of model suspensions in pressure driven and drag shear flows was performed priory 2D flow mapping. The flow behaviour of shear-thinning and shear-thickening model suspensions was analyzed in drag shear experiments using rotational rheometer and pressure driven shear flows using UVP-PD technique (e.g. Ouriev, 2000). From such experiments a variety of rheological and flow information was derived and used for further comparison between pressure driven and drag shear flows of highly concentrated suspensions.

2. EXPERIMENTAL SET-UP AND INSTRUMENTATION

Using a time averaged flow mapping the flow of shear-thinning and shear-thickening suspensions through a cylindrical contraction was investigated. In Fig. 1 a schematic of the setup to investigate the entrance region is illustrated. It consists of two basic components for pressure measurement and velocity visualization. The geometry is equipped with micro-pressure transducers for direct pressure measurement of the steady state flow in the upstream section. At the walls of the upstream tube the two UVP transducers were installed opposite to each other. Note that y-axis denotes here the radial direction across the measuring cell and x-axis denotes the flow direction, along the measuring cell axis. Thus, V_y denotes the velocity in radial direction and V_x is the velocity in flow direction. The velocity profiles were obtained along the measuring line Pm of the ultrasonic sensor (see Fig. 1 and Table 1).

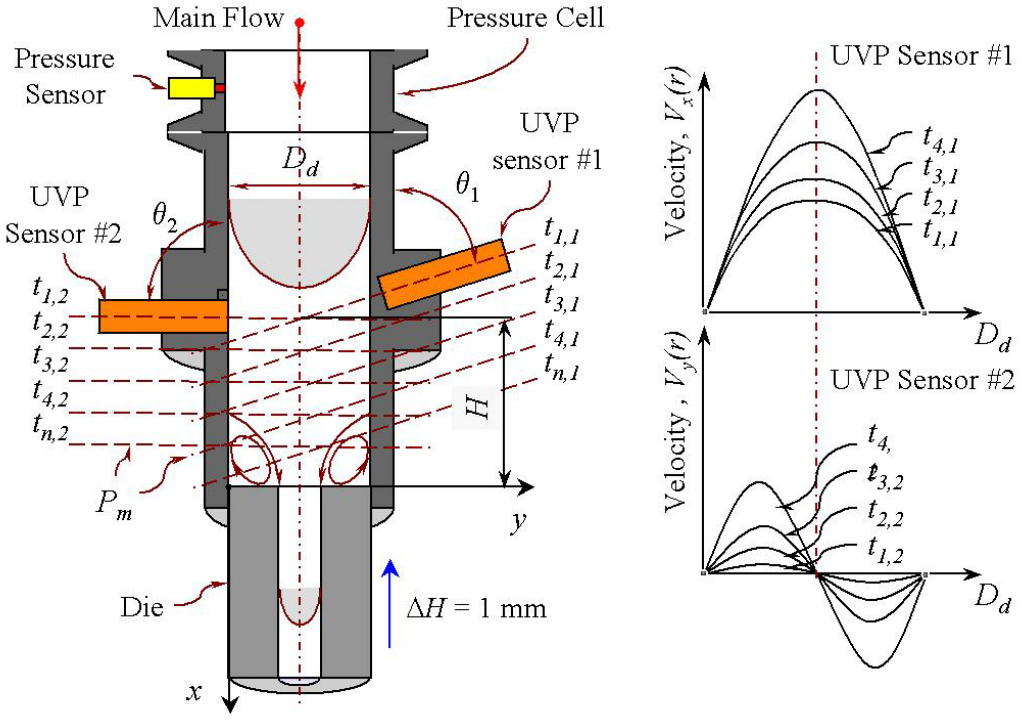

Fig. 1: Schematics of measuring cell and illustration of measuring procedure for 2D velocity mapping of converging flow.

The radial velocity $V_y\,(P_m)$ was measured using UVP sensor #2 and velocity profiles $V_x\,(P_m)$ in flow direction were obtained with UVP sensor #1 (see Fig. 1), where D_d is diameter of upstream section. For conversion of the velocity in flow direction, the results obtained from sensor #1 was multiplied by a factor of $1/\cos\theta$, where θ is the Doppler angle. The absolute velocity was not corrected if measured with the UVP sensor #2. In this case the Doppler angle is $\theta_2 = 90°$ ($1/\cos\theta_2 = 1$). The dimensions of the flow adapter $D_d = 23$ mm and $D_{DIE} = 4$, 6 and 8 mm, where D_{DIE} is die diameter. Consequently, the ratio between die diameter and inner diameter of the upstream tube varied between 2.87 and 5.27.

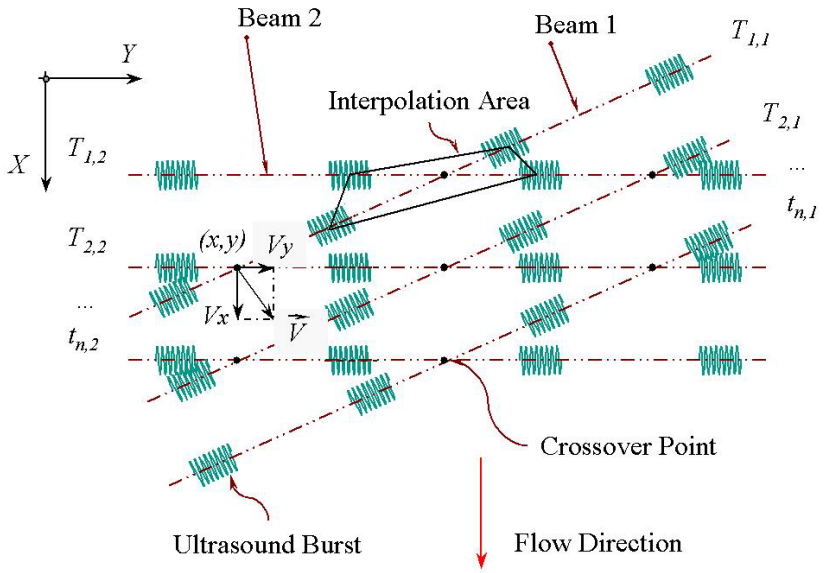

Fig. 2: Principle of 2D time averaged flow mapping.

Since the ultrasonic transducers have a direct contact to the fluid sample. The location of the sensor front was optimized in order to avoid a disturbance of the flow field around the sensor front. As shown in Fig. 1, the die entry was moved from the lowest position upper position H in steps of $\Delta H = 1$ [mm]. As shown in Fig. 2, time averaged flow map was obtained from the crossings of the ultrasonic beams of both UVP sensors. As already mentioned, the starting point of the scanning procedure was at the lowest die entry position (see Table 1). This sensor was installed with the Doppler angle $\theta_2 = 90°$ and was used for recording velocities in the radial direction $V_y(P_m) \equiv V_y(D_d)$. The dimensions of the sensor housing limited the minimum distance between the die entry and the UVP sensor #2. Having a sensor diameter of 8 mm, the shortest distance between the center of the acoustic beam and the die entry was 4 mm. The velocity in flow direction was visualized using UVP sensor #1 which was installed with an incline of $\theta_1 = 70°$ (Doppler angle) to the flow direction of the mainstream.

Table 1: Dimensions of the measuring cell

Parameter	[mm]	*Comments*
L_{DIE}	30	Length of the die
D_{DIE}	4, 6 and 8	Inner diameter of the die
D	23	Inner diameter of the upstream flow channel
θ_1	70	Doppler angle of UVP sensor #1
θ_2	90	Doppler angle of UVP sensor #2
H_{max}	70	Maximum distance between die entry and center of the UVP sensor #2
H_{min}	4 to 5	Minimal distance between die entry and center of the UVP sensor #2

As already mentioned above, priory to entrance flow velocity mapping a reference measurement of the steady pressure driven shear flow velocity profile was obtained. The aim

of this measurement is to obtain an averaged velocity profile for further evaluation of the profile shape symmetry around the tube axis and calculation of the volumetric flow rate Q_{UVP}. This was performed simultaneously with the pressure sensor calibration. As mentioned above, priory 2D flow visualization, the concept of the UVP-PD measuring technique was used beside volumetric flow rate measurement. The shear viscosity function, wall slip velocity and yield value. Detailed description of UVP-PD technique is given in work of Ouriev (2000).

The following methodology was applied for measurement and computation of the entrance flow for highly concentrated suspensions.

- Measurement of time averaged velocity profiles $V_x\,(P_m)$ and $V_y\,(P_m)$.
- Control of boundary flow conditions using instantaneous pressure and velocity information
- Volumetric flow rate computation from the velocity profile $V_x\,(P_m)$ of laminar pressure driven shear flow at maximum distance H. The result of this measurement was compared with the reference volume flow rate calculated from measured online mass flow rate and the sample's density.
- Calculation of time averaged flow map of entrance flow.

In present work only 8 mm diameter die is considered. Detailed discussion of experiments with 4 and 6 mm dies is given in work of Ouriev (2000).

3. MATERIALS

General information about shear-thinning and shear-thickening suspensions chosen for flow mapping is summarized in Table 2. The following parameters were chosen for characterization of the suspension sample: concentration of solids φ_{Sl} (by weight), shear viscosity at upper Newtonian plateau η_∞, maximum flow velocity Vy_{MAX} and volumetric flow rate Q_{UVP}.

Table 2: Highly concentrated suspensions of native cornstarch in Newtonian fluid matrix used in flow mapping experiment (T = 25°C ± 0.1°C).

Suspension	D_{DIE} [mm]	φ_{Sl} [%w]	η_∞ [mPas]	Re [-]	Vy_{MAX} [mm/sec]	Q_{UVP} [1] [l/h]
* Shear-thinning	8	40	51.4	192.76	543	590.8
* Shear-thickening			159.4	60.61	690.74	558.5

* Both suspensions consist of Newtonian fluid matrix of equal shear viscosity level, $\eta = 10$ *[mPas]*.

[1] For shear-thickening suspensions the volumetric flow rate is corrected with the wall slip velocity using UVP-PD method.

Flow of suspension sample was stationary and developed throughout the scanning procedure. Such flow conditions were controlled by means of Standard Mean Deviation (*SMD*) of absolute flow velocity and absolute pressure signals (e.g. Ouriev 2000).

According to observations described in work of Ouriev (2000), fully developed pressure driven shear flow of shear-thickening suspensions shows a strong effect of dilatancy at solids concentration above 30 %w. In this case the flow is accompanied by slip of the suspension

sample at the tube wall. Therefore a correction of volumetric flow rate was performed beside wall shear rate and finally viscosity slip correction (see Table 2).

4. RESULTS

4.1 2D Flow Mapping of highly concentrated suspensions

The flow map was obtained from the velocity vectors located in crossing points of two grid systems (see Fig. 2). One grid is based upon time-space positions of UVP sensor #2 beam.

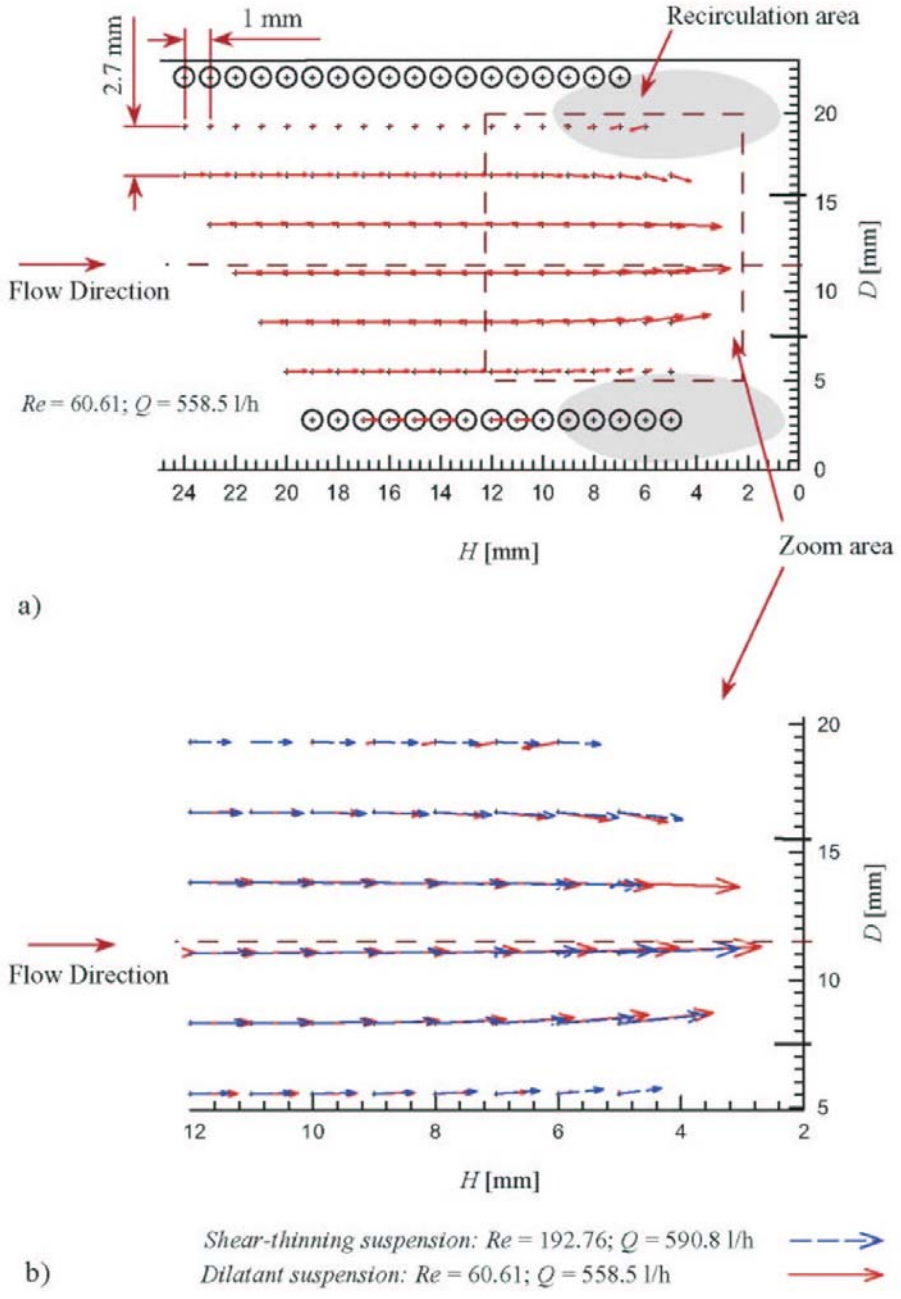

Fig. 3: Velocity map of the converging flow approaching a 8 mm die: a) flow map of shear-thickening suspension of starch φ_S = 40 % in GlS50; b) comparison between flow maps of shear-thinning (starch φ_S = 40 %w suspended in AK10) and shear-thickening (starch φ_S = 40 %w in GlS 50) suspensions.

1D velocity profiles were recorded along the ultrasound beam, P_m, at different axial positions H with displacement ΔH kept within 1 ± 0.015 mm (see Fig. 1 and Fig. 2). The second grid is obtained from displacement of the UVP sensor #1 beam inclined to the mainstream direction. The detailed information about the scanning procedure and grid design is given in work of Ouriev (2000).

The results of time averaged flow mapping are shown in Fig. 3a, a 2D-flow map of the shear-thickening suspension of 40 %w starch in GlS50 is shown. The comparison between the flow maps is illustrated in the enlarged Fig. 3b.

According to observations of Boger (1987), the vortex growth for shear-thinning fluids increases with increase of sample elasticity at given volumetric flow rate. For shear-thinning suspension, which is treated as viscous fluid, no secondary flow area (vortex) was observed. Contrarily to shear-thinning suspensions, shear-thickening suspensions showed large secondary flow area (see Fig. 3). Such increase of vortex at low *Re* and higher viscosity level (see Table 2) in comparison with shear-thinning suspension points appearance of viscoelastic properties of shear-thickening suspension in elongation flow.

According to comparison between shear-thinning and shear-thickening suspensions shown in Fig. 3b, it is noticed that the centerline velocity is higher for the shear-thickening suspension compared to the shear-thinning suspension, though the volumetric flow rate of shear-thinning suspension slightly larger compare to the shear-thickening suspension (see Table 2). The flow patterns shows a broader vortex boundary in case of shear-thinning suspension compare to the flow pattern of shear-thickening suspension. Likewise, the first sign of the vortex boundary is located at a distance of 9 mm above the die entry for shear-thickening suspension. No secondary flow regime was found down to the scanning area limit at 5 mm above the die entry in flow of shear-thinning suspensions.

5. CONCLUSIONS

From the results of introduced UVP 2D flow mapping the following advantages and disadvantages are concluded.

- Method works in Non-transparent and highly concentrated fluids of non-Newtonian type.
- High-resolution flow map was generated. In present work the dimensions of the mash elements reduced to 2.7 x 1 mm area (see Fig. 3) at given UVP sensor housing of 8 mm in diameter.
- Applicable to small channel dimensions of any geometry has been successfully tested.
- SMD (Standard Mean Deviation) of time averaged flow velocity profiles was used for control of flow conditions.
- Introduced scanning procedure assume stationary and developed flow. Pulsating flow can not be measured.
- Lost of velocity information close to the pipe walls due to the UVP starting depth restrictions (e.g. Ouriev 2000).
- Acoustic dissipation by means of strong scattering of ultrasound energy reduces velocity information which can be used for flow mapping. Lost of velocity data close to the opposite to UVP sensor location wall.
- Area of the secondary flow (Vortexes) could not be measured due to limitation of the lowest position above the die entry.
- Limitation of the maximum measurable velocity Vx_{MAX}. An overflow of velocity data at UVP Monitor could be observed due to exponential increase of Vx_{MAX} while approaching die entry.

Introduced technique could find a wide application field in industrial processes as: mixing, pipe transport, extrusion and etc., where extensional flows are dominating and desired to be characterized and controlled. It would be also of advantage to improve this technique and to step in real time flow mapping besides solving mentioned above disadvantages. In contrast to time averaged flow mapping where only stationary and developed flows can be considered; the real time flow mapping will be of advantage if non-stationary, pulsating flows must be investigated.

The results of fundamental research on model highly concentrated suspensions gave a sufficient background for further development of the UVP based in-line rheometry for industrial applications at Bühler AG.

6. ACKNOWLEDGMENTS

The author wishes to thank Prof. Windhab and Prof. Takeda, ETH LMVT workshop and Mr. Gogniat for their help.

7. REFERENCES

Ouriev, B., (2000) Ultrasound Doppler Based In-line Rheometry of Highly Concentrated Suspensions. PhD Thesis, ISBN: 3-905609-11-8, Zurich.

Ouriev, B., Koller, S., Korvink. J., Baltes, H., Windhab, E., (1995) On-Line Rheometry with Microsensors. ETH ILW-VT and ETH PEL Report, Zurich

Ouriev, B., Windhab, E., (1998) In-line rheological measurements and flow visualization using Doppler ultrasound method. 5th Europ. Rheo. Conf., Ljublijana, Slovenia

Ouriev, B., Windhab, E., (1998) On-line rheological measurements and process monitoring with flow visualization of non-transparent highly concentrated multiphase systems using Doppler ultrasound method. Intern. Conf. on Colloid Chem. and Phys.-Chem. Mechanics, Moscow, Russia

Ouriev, B., Windhab, E., (1999) Rheological Investigation of Concentrated Suspensions using a Novel In-line Doppler Ultrasound Method. Colloid Journal, Vol. 62 (2)

Ouriev, B., Windhab, E., (2002) Experiments in Fluids, Vol. 32, p. 204

Takeda, Y., (1986) Int. J. Heat Fluid Flow, Vol. 7, p. 313.

Takeda, Y., (1986) Velocity Profile Measurement by Ultrasound Doppler Shift Method. Int. J. Heat Fluid Flow 7 (4): 313.

Takeda, Y., (1991) Development of an Ultrasound Velocity Profile Monitor. Nuclear Engineering and Design 126 (2): 277-284.

Takeda, Y., (1995) Experimental Thermal and Fluid Science J., Vol. 10, no. 4, 444-453.

Takeda, Y., (1995) International Journal Series B-Fluids and Thermal Engineering, Vol. 38, no. 1, p. 8.

Takeda, Y., J., (1999) Experiments in Fluids, Vol. 26, no. 3, p. 177.

Uriev, N.B., (1980) Highly concentrated disperse systems, Khimiya, Moscow, p. 320

Uriev, N.B., (1980) Dynamics of structure of concentrated disperse systems. Physico-chemical mechanics and leofilic properties of dispers systems, Naukova Dumka, Kiev, pp. 3-12

Uriev, N.B., (1988) Physico-chemical Fundamentals of the Technology of Disperse Systems and Materials, Khimiya, Moscow, p. 256

Uriev, N.B., (1992). Structure, rheology and stability of concentrated disperse systems under dynamic conditions. J. of Colloids and Surfaces, 87, pages 1-4.

Windhab, E., (1986) Untersuchungen zum rheologischen Verhalten konzentrierter Suspensionen. Thesis VDI,

Windhab, E., Ouriev B; Wagner T; Drost M (1996) Rheological study of non-Newtonian fluids. 1st Inter. Symp. on Ultrasonic Doppler Methods for Fluid Mechanics and Fluid Engineering, PSI Villigen, Switzerland